THESIS

THREE GUANYLYL CYCLASES IN THE GREEN SHORE CRAB, *CARCINUS MAENAS:* cDNA CLONING AND EFFECTS OF MOLT STAGE ON EXPRESSION IN MOLTING GLAND (Y-ORGAN)

Submitted by

Jennifer L. Gunderson

Department of Biology

In partial fulfillment of the requirements

For the Degree of Master of Science

Colorado State University

Fort Collins, Colorado

Summer 2010

COLORADO STATE UNIVERSITY

June 16th, 2010

WE HEREBY RECOMMEND THAT THE THESIS PREPARED UNDER OUR SUPERVISION BY JENNIFER GUNDERSON ENTITILED THREE GUANYLYL CYCLASES IN THE GREEN SHORE CRAB, *CARCINUS MAENAS:* cDNA CLONING AND EFFECTS OF MOLT STAGE ON EXPRESSION IN THE MOLTING GLAND (Y-ORGAN) BE ACCEPTED AS FULFILLING IN PART REQUIREMENTS FOR THE DEGREE OF MASTER OF SCIENCE.

Committee on Graduate Work

Ronald B. Tjalkens

Anireddy N. Reddy

Advisor: Donald L. Mykles

Department Chair: Daniel R. Bush

ABSTRACT FOR THESIS

THREE GUANYLYL CYCLASES IN THE GREEN SHORE CRAB, *CARCINUS MAENAS:* cDNA CLONING AND EFFECTS OF MOLT STAGE ON EXPRESSION IN THE MOLTING GLAND (Y-ORGAN)

YO ecdysteroidogensis is suppressed by molt-inhibiting hormone (MIH) and the pleiotropic neuropeptide crustacean hyperglycemic hormone (CHH) with these neuropeptides being produced in the X-organ of the eyestalk (ES) ganglia. CHH signaling is mediated by a membrane receptor guanylyl cyclase (GC), while MIH signaling may involve a soluble NO-sensitive GC. Here we report the cloning of cDNA sequences encompassing the catalytic domain of the β subunit of a soluble NO-sensitive GC (*Cm-GC-Iβ*), membrane receptor GC (*Cm-GC-II*), and soluble NO-insensitive GC (*Cm-GC-III*) from the European green crab, *Carcinus maenas*, using RT-PCR and RACE. Adult *C. maenas* occur as two color morphs that differ in growth traits; the "green" morphs molt more frequently than the "red" morphs. These data suggest that YOs in red morphs are less active than the YOs in green morphs, and that the red morphs are refractory to molt induction by eyestalk ablation (ESA). We tested the effects of ESA on the expression of NO synthase (*Cm-NOS*), *Cm-GC-Iβ*, *Cm-GC-II*, and *Cm-GC-III* in the YOs from green and red morphs using quantitative PCR. Elongation factor-2 (*Cm-*

EF2) served as a constitutively expressed control. ESA caused a small, transient increase in hemolymph ecdysteroid titers in both morphs, with the increase occurring at 3 days post-ESA in green morphs and at 14 days post-ESA in red morphs. ESA had no significant effect on the expression of *Cm-EF2*, *Cm-NOS*, *Cm-GC-II*, and *Cm-GC-III*, which were not correlated with hemolymph ecdysteroid titers. ESA caused a significant decrease in *Cm-GC-Iβ* expression in red morphs, but had no significant effect in green morphs. Expression was also quantified in green morphs undergoing spontaneous natural molting. There was no significant difference in the expression of *Cm-EF2*, *Cm-NOS*, *Cm-GC-II*, and *Cm-GC-II* in YOs from intermolt, premolt, and postmolt animals. By contrast, *Cm-GC-III* mRNA was about 2-fold greater in YOs from postmolt animals than in intermolt and premolt animals. The results show that both color morphs are resistant to ESA and that molting has little effect on NOS and GC expression.

Jennifer Loreen Gunderson
Department of Biology
Colorado State University
Fort Collins, CO 80523
Summer 2010

INTRODUCTION

The process of ecdysis, or molting, in crustaceans requires precise coordination of physiological processes occurring in various organs and tissues, such as the degradation of the old exoskeleton, synthesis of a new exoskeleton, regeneration of lost appendages, and atrophy of skeletal muscle in the claws (Skinner, 1985). The molt cycle is divided into four major stages: intermolt, premolt, ecdysis, and postmolt (Skinner, 1985). Molting steroid hormones, or ecdysteroids, which are synthesized and secreted by a pair of molting glands, or Y-organs (YOs), initiate and coordinate these processes (Lachaise et al., 1993; Skinner, 1985). Thus, the YOs, located in the anterior cephalothorax, are activated to initiate the transition from the intermolt stage to the premolt stage. Hemolymph ecdysteroid levels are low during postmolt and intermolt stages, and increase during premolt, reaching a peak at the end of premolt (Chang, 1989; Skinner, 1985). There is a large drop in ecdysteroid level a few days before ecdysis, which serves as a trigger for actual shedding of the exoskeleton (ecdysis), as well as the growth of the claw muscles and the synthesis and calcification of the exoskeleton during the postmolt stage (Skinner, 1985).

The YOs are controlled by inhibitory neuopeptides produced by the X-organ/sinus gland (XO/SG) complex located in the eyestalks of decapod crustaceans (Chang, 1989; Lachaise et al., 1993; Skinner, 1985). These neuropeptides, molt-inhibiting hormone (MIH) and crustacean hyperglycemic hormone (CHH), inhibit ecdysteroidogenesis in the YO (Webster, 1998). Both of these neuropeptides share similar highly conserved motifs (Webster, 1991), and inhibit ecdysteroid synthesis via cGMP-dependent signaling pathways (Covi et al., 2009). CHH is a pleiotropic neuropeptide that regulates glucose

utilization, molting, osmoregulation, and metabolism (Chang et al., 1990; Khayat et al., 1998; Santos and Keller, 1993; Serrano et al., 2003; Yasuda et al., 1994). There are two isoforms of CHH produced by alternative splicing (Dircksen et al., 2001; Gu and Chan, 1998; Lee et al., 2007a; Soyez et al., 1994; Yang et al., 1997; Yasuda et al., 1994). The eyestalk CHH isoform inhibits the YO through a membrane-bound guanylyl cyclase, or GC-II (Goy, 1990; Pavloff and Goy, 1990). MIH signaling pathway may involve a soluble NO-dependent guanylyl cyclase (GC-I) (Covi et al., 2008; Mykles et al., 2010). Thus, CHH and MIH inhibit YO ecdysteroid biosynthesis through two distinct signaling pathways involving membrane receptor and NO-dependent GCs, respectively.

YO suppression through MIH has been proposed to involve nitric oxide (NO) activation of an NO-sensitive GC (GC-I) (Covi et al., 2008; Lee and Mykles, 2006; Mykles et al., 2010). cDNAs encoding a calmodulin (CaM)-dependent NO synthase (NOS) and three GCs have been cloned from the blackback land crab, *Gecarcinus lateralis* (Kim et al., 2004; Lee et al., 2007c). In addition, a cDNA encoding NOS in the European green crab has been cloned and characterized (McDonald et al., 2009). All four genes are expressed in the YO (Kim et al., 2004; Lee et al., 2007c; McDonald et al., 2009). GC-I is a heterodimer; the catalytic, or β, subunit has heme/NO-binding and heme/NO-binding-associated domains, which are characteristic of β subunits of NO-sensitive GCs in other species (Lee et al., 2007c). The GC-II has extracellular ligand-binding, transmembrane, cytosolic kinase homology, dimerization and catalytic domains (Lee et al., 2007c; Liu et al., 2004; Zheng et al., 2006). The GC-III is a soluble, NO-independent GC that resembles GC-II (Lee et al., 2007c). The data indicate that MIH signaling is composed of two phases. The "triggering" phase produces a rapid, transient

increase in cAMP, influx of Ca^{2+}, and binding of Ca^{2+} to CaM; the "summation" phase follows when Ca^{2+}/CaM activates NOS, which, in turn, activates GC-I and produces a large sustained increase in cGMP (Covi et al., 2008; Lee and Mykles, 2006; Mykles et al., 2010).

It is becoming apparent that there is a constant interaction between the XO/SG complex and the YO during the molt cycle. YOs from intermolt animals are most sensitive to MIH and CHH, which allow prolonged suppression of ecdysteroidogenesis, even at low circulating levels of MIH and CHH in the hemoymph. As the animal progresses through premolt, the YOs become less sensitive to CHH and MIH, but MIH titers in the hemolymph and MIH receptor numbers in the YO membrane do not decline during premolt (Chung and Webster, 2003; Chung and Webster, 2005; Nakatsuji and Sonobe, 2004; Sefiani et al., 1996), suggesting that the decrease in sensitivity to the neuropeptide is downstream from the receptor. Phosphodiesterase activity is correlated with reduced sensitivity during premolt, suggesting that the hydrolysis of cyclic nucleotides is involved (Nakatsuji et al., 2009; Nakatsuji et al., 2006). However, the increase in phosphodiesterase activity cannot account fully for the magnitude in the reduced response to MIH (Nakatsuji et al., 2006), indicating that additional components of the signaling pathway are down-regulated during premolt. If NOS and/or GC-Iβ are involved in MIH signaling, the down-regulation of one or both could contribute to the reduced response of MIH by making the YO less sensitive to MIH. Conversely, up-regulation of NOS and/or GC-Iβ during intermolt could contribute to increased sensitivity to MIH.

Adults of the European green crab, *Carcinus maenas*, occur as two color morphs in wild populations that differ in ecophysiological traits. The two color morphs are distinguished by the color of the arthrodial membrane articulating the basal segments of each of the legs; "green" morphs have a clear or greenish joint and "red" morphs have an orange or red joint (McGaw et al., 1992; McGaw and Naylor, 1992a). Red morphs are found primarily in the subtidal zone and they cannot tolerate low salinity for extended periods (McGaw et al., 1992; McGaw and Naylor, 1992a; McGaw and Naylor, 1992b). Green morphs are more prevalent in the high intertidal zone and salt marshes and can tolerate greater ranges in salinity (McGaw et al., 1992; McGaw and Naylor, 1992a; McGaw and Naylor, 1992b). Red morphs have a thicker carapace and molt less frequently than green morphs (Reid et al., 1997). Green color morphs direct more energy into molting and growth, while red morphs direct more energy to reproduction (Reid et al., 1997). *C. maenas* has invaded the harbor at Bodega Bay, California. Our own observations are that the color morphs vary by season. Green morphs are more common during the winter months and molt in late winter and early spring. After molting, the green morphs transition to the red color morph, which are more common during summer. This transition is accelerated by eyestalk ablation (Mykles, unpublished data).

Acute molt induction by eyestalk ablation (ESA) up-regulates expression of NO signaling components in the YOs of green morphs of *C. maenas* (*Cm-NOS*) and blackback land crabs, *Gecarcinus lateralis* (*Gl-NOS*, *Gl-GC-Iβ*, and *Gl-GC-III*). ESA increases *Cm-NOS*, *Gl-NOS, Gl-GC-Iβ* and *Gl-GC-III* expression, which is correlated with hemolymph ecdysteroid titers (Lee et al., 2007b; McDonald et al., 2009). ESA has no significant effect in *Gl-GC-II* mRNA levels and there is no significant correlation

between *Gl-GC-II* mRNA transcript levels and hemolymph ecdysteroid concentrations (Lee et al., 2007b; McDonald et al., 2009). As red morphs molt less frequently than green morphs, we hypothesized that *GC-Iβ*, *GC-II*, and *GC-III* are differentially expressed in the YOs. The YOs in red morphs may be in an inactivated state, thus making red morphs refractory to molt induction by ESA. The YOs in green morphs respond to ESA (McDonald et al., 2009), indicating that YOs can be activated by acute withdrawal of eyestalk neuropeptides. Here we report the cloning of sequences encompassing the catalytic domains of the *GC-Iβ, GC-II,* and *GC-III* genes in the European green crab, *Carcinus maenas*, using RT-PCR and RACE. The purpose of this study was to (1) compare the effects of ESA on the expression of *Cm-NOS*, *Cm-GC-Iβ, Cm-GC-II,* and *Cm-GC-III* in red and green morphs and (2) quantify *GC* and *NOS* expression in green morphs undergoing spontaneous molts. The results show that both color morphs are resistant to ESA and that molting has little effect on NOS and GC expression.

MATERIALS AND METHODS

Animals

European green crabs (*Carcinus maenas*) were collected from the harbor at Bodega Bay, California. They were maintained under ambient conditions in the facilities of Bodega Marine laboratory or were shipped to Colorado. In Colorado, animals were kept in aerated 30 ppt Instant Ocean (Aquarium Systems, Mentor, OH, USA) at 20°C and fed cooked chicken liver twice a week. Water was changed twice a week (or more if water became cloudy or there was a death in the cage). A 12h:12h dark:light cycle was used. Eyestalk ablation (ESA) was used to activate the YO (Skinner, 1985). Hemolymph

ecdysteroid concentration was quantified by ELISA (Kingan, 1989). Animals undergoing natural molts were collected in February and March, 2010.

Cloning of Cm-Guanylyl cylcases (Cm-GC)

RT-PCR and Rapid Amplification of cDNA Ends (RACE) were the cloning techniques used to obtain *Cm-GCIβ, Cm-GCII,* and *Cm-GCIII*. An initial partial cDNA sequence for *Cm-GCIβ*, *Cm-GCII,* and *Cm-GCIII* was attained by designing primers to a highly conserved region (catalytic domain) of the land crab, *Gecarcinus lateralis* (*Gl*), guanylyl cyclases (Lee et al., 2007c). A mixed tissue cDNA template (including YO, claw, and thoracic ganglia) was used for the initial PCR. The PCR conditions included an initial 4 min denaturation at 96°C followed by 35 cycles of denaturation for 30 s at 96°C, annealing for 30 s at the appropriate melting temperature for the specific primer set, and extension for 30-90 s at 72°C. Extension time varied with expected product size allowing 30 s for every 500 bp. PCR reaction consisted of 1 µl cDNA template, 0.5 µl each forward and reverse primers (Table 1), 5 µl GoTaq Green Master Mix (Promega Corp., Madison, WI, USA), and 3 µl sterile deionized water (Integrated DNA Technology). Reactions were performed using a Veriti 96 Well Thermal Cycler (Applied Biosystems Inc., Foster City, CA, USA).

5'RACE and 3'RACE PCR used the FirstChoice RLM-RACE kit (Applied Biosystems/Ambion, Austin, TX, USA) as performed by McDonald et al. (2009). Nested primers were used to amplify products from the RACE templates. Outer reactions contained 1 µl 3' or 5' RACE template, 2 µl 3' or 5' RACE outer primer, 2 µl specific outer primer (Table 1), 14.25 µl GoTaq Green mix (Promega), and 30.75 µl nuclease free

water (Integrated DNA Technology). Inner reactions contained 1 µl outer 3' or 5' RACE reaction, 1 µl specific inner primer (Table 1), 1 µl 3' or 5' RACE inner primer, 5 µl GoTaq Green mix (Promega), and 2 µl nuclease free water. PCR conditions were 3 min denaturation at 94 °C, followed by 35 cycles of 30 s at 94 °C, 30 s at 60°C, 1 min 30 s at 72 °C, and a final extension of 7 min at 72 °C. PCR products were separated using 1.0% agarose gel electrophoresis and stained with ethidium bromide. The gel slices were purified using Qiaex II Gel Extraction kit (Qiagen, Inc., Valencia, CA, USA) and DNA was ligated into pJet 1.2 (Fermentas) vector which was transformed into CH3 Blue (Bioline USA Ins., Taunton, MA, USA) *E. coli* cells. Plasmids were purified using QAIprep Spin Miniprep kit (Qiagen) and sequenced using pJET sequence-specific primers (Davis Sequencing, Davis, CA, USA).

RNA isolation and quantitative real-time RT-PCR

The RNA isolation protocol followed that of Covi et al. (2010). Green crabs were anesthetized by ice for 5 min prior to dissection of the Y-organ (YO). Hemolymph samples (100 µl) were also taken for quantification of ecdysteroids (Medler et al., 2005). YO tissues were frozen immediately in liquid nitrogen and stored at -80°C. Total RNA was isolated using TRIzol reagent (Invitrogen, Carlsbad, CA, USA) using manufacturer's protocol. In order to remove the genomic DNA from the sample, total RNA was treated with DNAase I for 30 min. Next, a phenol:chloroform:isoamyl alcohol extraction (25:24:1) was performed on the DNase treated RNA to remove the DNase, salts, and digested DNA. The total RNA was precipitated with 1 volume of isopropanol and dissolved in 30 µl of nuclease free water (Integrated DNA Technology). The

concentration of nucleic acid was determined by absorbance at 260 nm using NanoDrop ND-1000 Spectrophotometer (Thermo Fisher Scientific Inc). One microgram of DNase-treated RNA was used for a 20 µl cDNA synthesis reaction. Reactions contained 4 µl Transcriptor RT reaction buffer (Roche), 0.5 µl Ribolock RNase Inhibitor (40u/µl) (Fermentas), 0.5 µl Reverse Transcriptase (Roche), 2.0 µl dNTP (10 mM), and 5 µl nuclease free water. After the cDNA synthesis reaction, RNase H (New England Biolabs, Ipswich, MA, USA) was used to remove complementary RNA.

A Light Cycler Fast Start DNA Master Plus SYBR GREEN I reaction mix (Roche Applied Science) and a Light Cycler 480 thermal cycler (Roche Applied Science, Nutley, NJ, USA) was used for quantitative analysis of *Cm-GCIβ, Cm-GCII, Cm-GCIII,* and *Cm-NOS* (Genbank accession #GQ862349), and *Cm*-Elongation Factor-2 (*Cm-EF-2*; Genbank accession #GU808334). *Cm-EF-2* is a "housekeeping" gene that is constitutively expressed and served as the control for RNA isolation and cDNA synthesis. qPCR reactions consisted of 1 µl cDNA, 5 µl 2x SYBR Green Master Mix, 0.5 µl (10 mM) of both forward and reverse specific primers (Table 2), and 3 µl of PCR-grade water. The PCR conditions were an initial 95°C for 5 min, followed by 45 cycles of 95°C for 5 s (denaturation), 62°C for 5 s (annealing), and 72° for 20 s (extension). The melting temperature analysis of the PCR products and the concentrations of the PCR transcripts were conducted using Roche, version 1.2 Light cycler 480 software (Appendix I). Standard curves were prepared by serial dilutions of purified PCR product (10^{-8} ng/µl to 10^{-16} ng/µl) for *Cm-GCIβ, Cm-GCII, Cm-GCIII, Cm-NOS,* and *Cm-EF-2*. PCR products were purified using Qiaex II Gel Extraction kit.

Statistical analysis was performed using JMP 5.1.2 software (SAS institute, Inc., Cary, NC, USA). All qPCR data was log transformed to reduce the variance of the mean. *Cm-GCIβ, Cm-GCII, Cm-GCIII,* and *Cm-NOS* data was normalized to *Cm-EF-2* data. The normalization ratio was calculated by taking each *Cm-EF2* sample copy number and dividing by the average *Cm-EF2* copy number (3.00×10^7; n=75). *Cm-GCIβ, Cm-GCII, Cm-GCIII,* and *Cm-NOS* copy numbers were divided by the normalization ratio to obtain the normalized data. Means for transcript abundance were compared using an analysis of variance (ANOVA) for days post-ESA verses log copy number. An ANOVA was also used to compare the means of naturally molting animals in various molting stages verses log copy numbers. A paired t-test was used to compare the means for transcript abundance between red and green morph hemolymph ecdysteroid concentration verses log copy number. A Grubb's test (extreme studentized deviate) was used to detect outliers. The level of significance for the all the data analyses was set at $\alpha=0.05$.

RESULTS

Cloning of Cm-NOS, Cm-GCIβ, Cm-GCII, and Cm-GCIII

An initial PCR product (~230 bp) amplified using degenerate primers was ligated into a vector and cloned. Transformed colonies were selected and grown; plasmids were purified from each clone and sequenced. Three distinct sequences were obtained that corresponded to *G. lateralis* GC-Iβ, GC-II, and GC-III (Fig 1, 2. A, 3). The *Cm-GC-Iβ* and *Cm-GC-III* 3'UTR were obtained 3' RACE. Nested 3' RACE PCR with sequence specific primers (Table 1) directed toward each of the three obtained sequences resulted in the remainder of the 3' ORF and the 3'UTR of the *Cm-GC-Iβ* and *Cm-GC-III* (Fig 1,

3). Nested 3' RACE failed to amplify the remainder of the *Cm-GC-II*, but additional downstream sequence was obtained from sequence specific forward primers (Table 1) when the RLM-RACE kit reverse primer apparently annealed to an A-rich sequence in the ORF (Fig 2 B). Additional 5' sequence for *Cm-GC-III* was amplified using sequence-specific *Cm-GC-II* gap bridging primers (Table 1). The *Cm-GC-II* primer sequences and *Cm-GC-III* cDNA sequence apparently were similar enough to allow annealing of the primers to the *Cm-GC-III* cDNA. Nested 5' RACE PCR failed to obtain the 5' UTR of *Cm-GC-II* and *Cm-GC-Iβ*, which was most likely due to the predicted length (~2100 bp and ~1600 bp, respectively), based on the *G. lateralis* GC sequences. Difficulty in transforming DNA fragments larger than 400 bp resulted in a suspension of the *Cm-GC-Iβ, Cm-GC-II,* and *Cm-GC-III* cloning. The partial cDNA sequences of *Cm-GC-Iβ, Cm-GC-II,* and *Cm-GC-III* were homologous to *Gl-GC-Iβ, Gl-GC-II,* and *Gl-GC-III*. *Cm-GC-Iβ* shared 97% amino acid identity with *Gl-GCIβ* (Fig 4). The upstream sequence of *Cm-GC-II* shared 60% identity with *Gl-GC-II*, while the downstream sequence of *Cm-GCII* shared 78% identity with *Gl-GCII* (Fig 5). *Cm-GC-III* shared 85% identity with *Gl-GC-III* (Fig 6).

Effect of eyestalk ablation on hemolymph ecdysteroid concentration and NOS, GC-Iβ, GC-II, and GC-III expression in Y-organs of red and green morphs

ESA caused a transient increase in hemolymph ecdysteroid titers, but the magnitude and timing of the increase differed between the two color morphs. In red morphs, there was a 4.2-fold increase ($P = 0.0001$) in ecdysteroid concentration between day 3 and day 14 post-ESA, which was followed by a 3.8-fold decrease ($P = 0.0001$) between day 14

and day 21 post-ESA (Fig 7). In green morphs, a 2-fold increase ($P = 0.012$) in hemolymph ecdysteroid occurred at 3 days post-ESA (Fig 7).

ESA had no significant effect on the expression of *Cm-EF2*, which served as a constitutively expressed control, in green and red morphs (Fig 8 A). Moreover, *Cm-EF2* mRNA levels were not significantly correlated with hemolymph ecdysteroid concentration in red ($P > 0.1$) or green ($P > 0.23$) morphs (Fig 8 B). ESA had no significant effect on the expression of *Cm-NOS* in either the red or green morph (Fig 9 A). In addition, there were no significant correlations between *Cm-NOS* mRNA levels and hemolymph ecdysteroid concentrations in either morph (Fig 9 B).

ESA had a small, but significant, effect on *Cm-GC-Iβ* expression in red morphs, but not in green morphs. There was a significant difference between the means of day 4 and 14 post-ESA in the red morphs *Cm-GC-Iβ* expression; the mean at day 14 was 1.6-fold ($P = 0.0214$) less than day 4 (Fig 9 C). There were no significant differences in the means of green morphs when data were analyzed as a function of days post-ESA (Fig 9 C). *Cm-GC-Iβ* mRNA levels were negatively correlated ($P = 0.0138$) with hemolymph ecdysteroid concentration in the red morphs, but there was no correlation within the green morphs (Fig 9 D).

There was no significant effect of ESA on the expression of *Cm-GC-II* and *Cm-GC-III* in either color morph (Fig 9 E, G). Moreover, mRNA levels of *Cm-GC-II* and *Cm-GC-III* were not significantly correlated with hemolymph ecdysteroid concentrations in either red or green morph (Fig 9 F, H).

Effect of molt stage on Cm-NOS, Cm-GC-Iβ, Cm-GC-II, and Cm-GC-III in naturally molting green morphs

Animals (green morphs) captured during late winter and early spring underwent spontaneous molting. YOs were harvested from animals at intermolt (stage C_4), premolt (stage D_1), and postmolt (3-5 days after ecdysis) stages. Molt stage had no significant effect on the expression of *Cm-NOS, Cm-GC-Iβ,* and *Cm-GC-II* (Fig. 10). By contrast, expression of *Cm-GC-III* varied with the molt cycle. Postmolt animals showed a 2-fold increase in *Cm-GC-III* mRNA level compared to intermolt ($P = 0.0201$) and premolt ($P = 0.0073$) animals (Fig 10).

DISCUSSION

Four types of GCs have been cloned and characterized in arthropods. GC-Iβ is an NO-sensitive soluble GC that forms a heterodimer of α and β subunits (Buechler et al., 1991; Harteneck et al., 1991; Hu et al., 2008). The catalytic subunit, GC-Iβ, has heme/NO-binding and heme/NO-binding-associated domains (Nighorn et al., 1998). A membrane receptor GC, *Gl-GC-II*, has signal peptide, N-terminal extracellular ligand-binding, transmembrane, kinase homology, dimerization, and catalytic domains (Lee et al., 2007c; Morton and Nighorn, 2003). GC-III is a soluble NO-insensitive GC that resembles GC-II, but lacks the signal peptide, ligand-binding, transmembrane, and most of the kinase homology domain (Lee et al., 2007c; Nighorn et al., 2001; Simpson et al., 1999). A GC-IV has also been identified in the hawk moth (*Manduca sexta*) (Nighorn et al., 1999). *GC-Iβ* and *GC-III* have been cloned in land crab and *GC-II* has been cloned in land crab, blue crab, and crayfish (Lee et al., 2007c; Liu et al., 2004; Zheng et al., 2006).

The partial cDNA sequences obtained from initial PCR using degenerate nested primers directed to the catalytic domain were grouped into three major classes based on sequence identities (Lee et al., 2007c). *Cm-GC-Iβ, Cm-GC-II,* and *Cm-GC-III* are orthologs of *Gl-GCIβ, Gl-GCII,* and *Gl-GCIII*, respectively, based on at least a 60% amino acid sequence identity between each class using sequence alignments.

To expand on the experiments performed by (McDonald et al., 2009) and (Lee et al., 2007b) on land crab and green crab NOS and land crab *GC-Iβ, GC-II,* and *GC-III*, the effects of ESA and molting on the expression of *Cm-GCIβ, Cm-GCII,* and *Cm-GCIII* in the YOs of red and green morphs was conducted. McDonald et al. (2009) found that NOS expression increases in both *G. lateralis* and *C. maenas* YOs by 32-fold for *Gl-NOS* at day 24 and by 5-fold for Cm-NOS by day 7 after ESA. *Gl-NOS* and *Cm-NOS* transcript numbers were correlated with hemolymph ecdysteroid levels (McDonald et al., 2009). In land crab, *Gl-NOS* and *Gl-GC-Iβ* transcript numbers are correlated with hemolymph ecdysteroid levels, suggesting that expression of these genes is associated with YO activation. *Gl-GC-Iβ* mRNA transcript number increases ~10-fold by 7 days post-ESA (Lee et al., 2007b). Here we report that *Cm-NOS* transcript levels and hemolymph ecdysteroid concentrations were non-responsive, which did not confirm the results of McDonald et al. (2009). The minimal or lack of response to ESA in both red and green morphs suggests that green crabs can become refractory to acute withdrawal of eyestalk neuropeptides induced by ESA and that the green crab YO may not upregulate eyestalk neuropeptide receptors as predicted.

Both Lee et al. (2007b) and McDonald et al. (2009) showed that ESA increases *Gl-GC-1β* expression in land crab YOs. By contrast, ESA did not have an effect on *C.*

maenus green morph *GC-Iβ* mRNA expression levels nor was there any correlation with hemolymph ecdysteroid levels. The means were not significantly different between the various days post-ESA animals for *Gl-GC-II* mRNA (McDonald et al., 2009). In addition, there was no significant correlation between *Gl-GC-II* mRNA and hemolymph ecdysteroid concentration (McDonald et al., 2009). Similarly, ESA did not have an effect on *Cm-GC-II* mRNA expression; *Cm-GC-II* expression levels had no correlation with hemolymph ecdysteroid levels (Fig 9 E, F). Additionally, ESA had no significant effect on expression of *Cm-GC-III* in (Fig 9 G). Figure 9 H illustrates there were no significant correlations between *Cm-GC-III* mRNA expression levels and hemolymph concentrations.

Both color morphs are resistant to ESA, as ESA caused only a small, transient increase in hemolymph ecdysteroid titers. ESA did not have any effect on *Cm-NOS, Cm-GC-II,* and *Cm-GC-III* transcript copy numbers in either red or green morph (Fig 9 A, E, G). Likewise, *Cm-NOS*, *Cm-GC-II*, and *Cm-GCIII* mRNA levels were not correlated with hemolymph ecdysteroid (Fig 9 B, F, H). This lack of hemolymph ecdysteroid change suggests that both red and green morph crabs can be resistant to ESA. There was a significant difference between the means of day 4 and 14 post-ESA in the red morphs *Cm-GC-Iβ* expression; the mean at day 14 was 1.6-fold less than day 4. By contrast, there was no significant effect on the green morph *Cm-GC-Iβ* expression (Fig 9 C). *Cm-GC-Iβ* was negatively correlated with hemolymph ecdysteroid concentration in red morphs, but there was no correlation within the green morphs (Fig 9 D). While *Cm-GC-Iβ* was somewhat affected by ESA, it is not near the same 10-fold magnitude of difference as that of Gl-*GC-Iβ* (Lee et al., 2007b).

ESA is used as an acute activation of the YO by the withdrawal of eyestalk neuropeptides. The multiplicity of responses to ESA observed in the green crabs suggests there is a difference between natural molting and acute stimulation of a premolt-like stage within the molting pathway. In naturally molting green morphs, *Cm-GC-III* mRNA levels increased ~2- fold from premolt to postmolt and ~2-fold increase from intermolt to postmolt (Fig 10). No other significant differences among *Cm-GC-Iβ, Cm-GC-II,* or *Cm-NOS* transcript levels in naturally molting green crabs were observed in intermolt, premolt, or postmolt. The discrepancy in *GC-Iβ* expression between naturally molting and ESA crabs gives more evidence to the difference between ESA and natural molting.

In conclusion, partial cDNA sequences were categorized as coding for *Cm-GC-Iβ, Cm-GC-II,* and *Cm-GC-III.* To expand on the experiments performed by McDonald et al. (2009) on land crab and green crab *NOS* and land crab *GC-Iβ, GC-II, GC-III* during the molting cycle, expression of *Cm-GC-Iβ, Cm-GC-II,* and *Cm-GC-III* mRNA transcript levels were collected from 0 to 24 days post ESA on red and green morphs. Due to the minimal or lack of response to ESA in both red and green morphs, it suggests green crabs can become refractory to acute induction by ESA and that the green crab YO may not upregulated eyestalk neuropeptide receptors as predicted.

Interestingly, naturally molting green morph *Cm-GC-III* mRNA transcript levels showed a significant increase from intermolt to postmolt and from premolt to postmolt. This significant increase in *Cm-GC-III* expression in only naturally molting animals suggests a difference between the acute and normal progression of neuropeptide withdrawal. It may also signify a greater role of *GC-III* in the molting cycle of green

crab. While red and green morphs appear to have differing geographic locations and behavioral actions in regard to mating (McGaw et al., 1992), they vary only slightly in GC expression with a solitary change in *GC-Iβ* expression between day 4 and 14 post ESA. Studies are currently being performed on 90 day post ESA YO samples to determine if green crab has a longer response time to the absence of eyestalk neuropeptides.

REFERENCES

Buechler, W.A., Nakane, M., Murad, F., 1991. Expression of soluble guanylate cyclase activity requires both enzyme subunits. Biochem. Biophys. Res. Commun. 174, 351-357.

Chang, E.S., 1989. Endocrine regulation of molting in Crustacea. Rev. Aquatic Sci. 1, 131-158.

Chang, E.S., Prestwich, G.D., Bruce, M.J., 1990. Amino acid sequence of a peptide with both molt-inhibiting and hyperglycemic activities in the lobster, *Homarus americanus*. Biochem. Biophys. Res. Commun. 171, 818-826.

Chung, J.S., Webster, S.G., 2003. Moult cycle-related changes in biological activity of moult-inhibiting hormone (MIH) and crustacean hyperglycaemic hormone (CHH) in the crab, *Carcinus maenas*. From target to transcript. Eur. J. Biochem. 270, 3280-3288.

Chung, J.S., Webster, S.G., 2005. Dynamics of *in vivo* release of molt-inhibiting hormone and crustacean hyperglycemic hormone in the shore crab, *Carcinus maenas*. Endocrinology 146, 5545-5551.

Covi, J., Gomez, A., Chang, S., Lee, K., Chang, E., Mykles, D., 2008. Repression of Y-organ ecdysteroidogenesis by cyclic nucleotides and agonists of NO-sensitive guanylyl cyclase. In: Morris, S., Vosloo, A. (Eds.), 4th Meeting of Comparative Physiologists & Biochemists in Africa - Mara 2008 - "Molecules to Migration: The Pressures of Life", Monduzzi Editore International, Bologna, Italy, pp. 37-46

Covi, J.A., Bader, B.D., Chang, E.S., Mykles, D.L., 2010. Molt cycle regulation of protein synthesis in skeletal muscle of the blackback land crab, *Gecarcinus lateralis*,

and the differential expression of a myostatin-like factor during atrophy induced by molting or unweighting. J. Exp. Biol. 213, 172-183.

Covi, J.A., Chang, E.S., Mykles, D.L., 2009. Conserved role of cyclic nucleotides in the regulation of ecdysteroidogenesis by the crustacean molting gland. Comp. Biochem. Physiol. 152A, 470-477.

Dircksen, H., Böcking, D., Heyn, U., Mandel, C., Chung, J.S., Baggerman, G., Verhaert, P., Daufeldt, S., Plösch, T., Jaros, P.P., Waelkens, E., Keller, R., Webster, S.G., 2001. Crustacean hyperglycaemic hormone (CHH)-like peptides and CHH-precursor-related peptides from pericardial organ neurosecretory cells in the shore crab, *Carcinus maenas*, are putatively spliced and modified products of multiple genes. Biochem. J. 356, 159-170.

Goy, M.F., 1990. Activation of membrane guanylate cyclase by an invertebrate peptide hormone. J. Biol. Chem. 265, 20220-20227.

Gu, P.L., Chan, S.M., 1998. The shrimp hyperglycemic hormone-like neuropeptide is encoded by multiple copies of genes arranged in a cluster. FEBS Lett. 441, 397-403.

Harteneck, C., Wedel, B., Koesling, D., Malkewitz, J., Bohme, E., Schultz, G., 1991. Molecular cloning and expression of a new alpha-subunit of soluble guanylyl cyclase. Interchangeability of the alpha-subunits of the enzyme. FEBS Lett. 292, 217-222.

Hu, X.H., Murata, L.B., Weichsel, A., Brailey, J.L., Roberts, S.A., Nighorn, A., Montfort, W.R., 2008. Allostery in recombinant soluble guanylyl cyclase from *Manduca sexta*. J. Biol. Chem. 283, 20968-20977.

Khayat, M., Yang, W.J., Aida, K., Nagasawa, H., Tietz, A., Funkenstein, B., Lubzens, E., 1998. Hyperglycaemic hormones inhibit protein and mRNA synthesis in in vitro-incubated ovarian fragments of the marine shrimp *Penaeus semisulcatus*. Gen. Comp. Endocrinol. 110, 307-318.

Kim, H.W., Batista, L.A., Hoppes, J.L., Lee, K.J., Mykles, D.L., 2004. A crustacean nitric oxide synthase expressed in nerve ganglia, Y-organ, gill and gonad of the tropical land crab, *Gecarcinus lateralis*. J. Exp. Biol. 207, 2845-2857.

Kingan, T.G., 1989. A competitive enzyme-linked immunosorbent assay - Applications in the assay of peptides, steroids, and cyclic nucleotides. Anal. Biochem. 183, 283-289.

Lachaise, A., Le Roux, A., Hubert, M., Lafont, R., 1993. The molting gland of crustaceans: localization, activity, and endocrine control (a review). J. Crustacean Biol. 13, 198-234.

Lee, K.J., Doran, R.M., Mykles, D.L., 2007a. Crustacean hyperglycemic hormone from the tropical land crab, *Gecarcinus lateralis*: cloning, isoforms, and tissue expression. Gen. Comp. Endocrinol. 154, 174-183.

Lee, S.G., Bader, B.D., Chang, E.S., Mykles, D.L., 2007b. Effects of elevated ecdysteroid on tissue expression of three guanylyl cyclases in the tropical land crab *Gecarcinus lateralis*: possible roles of neuropeptide signaling in the molting gland. J. Exp. Biol. 219, 3245-3254.

Lee, S.G., Kim, H.W., Mykles, D.L., 2007c. Guanylyl cyclases in the tropical land crab, *Gecarcinus lateralis*: Cloning of soluble (NO-sensitive and -insensitive) and membrane receptor forms. Comp. Biochem. Physiol. 2D, 332-344.

Lee, S.G., Mykles, D.L., 2006. Proteomics and signal transduction in the crustacean molting gland. Integr. Comp. Biol. 46, 965-977.

Liu, H.F., Lai, C.Y., Watson, R.D., Lee, C.Y., 2004. Molecular cloning of a putative membrane form guanylyl cyclase from the crayfish *Procambarus clarkii*. J. Exp. Zool. 301A, 512-520.

McDonald, A.A., Chang, E.S., Mykles, D.L., 2009. Comparative anaylsis of nitric oxide signaling in the crustacean molting gland. M.S. Thesis, Colorado State University.

McGaw, I.J., Kaiser, M.J., Naylor, E., Hughes, R.N., 1992. Intraspecific morphological variation related to the molt cycle in color forms of the shore crab *Carcinus maenas*. J. Zool. 228, 351-359.

McGaw, I.J., Naylor, E., 1992a. Distribution and rhythmic locomotor patterns of estuarine and open-shore populations of *Carcinus maenas*. J. Mar. Biol. Assoc. U. K. 72, 599-609.

McGaw, I.J., Naylor, E., 1992b. Salinity preference of the shore crab *Carcinus maenas* in relation to coloration during intermolt and to prior acclimation. J. Exp. Mar. Biol. Ecol. 155, 145-159.

Medler, S., Brown, K.J., Chang, E.S., Mykles, D.L., 2005. Eyestalk ablation has little effect on actin and myosin heavy chain gene expression in adult lobster skeletal muscles. Biol. Bull. 208, 127-137.

Morton, D.B., Nighorn, A., 2003. MsGC-II, a receptor guanylyl cyclase isolated from the CNS of *Manduca sexta* that is inhibited by calcium. J. Neurochem. 84, 363-372.

Mykles, D.L., Adams, M.E., Gäde, G., Lange, A.B., Marco, H.G., Orchard, I., 2010. Neuropeptide action in insects and crustaceans. Physiol. Biochem. Zool. in press.

Nakatsuji, T., Lee, C.Y., Watson, R.D., 2009. Crustacean molt-inhibiting hormone: Structure, function, and cellular mode of action. Comp. Biochem. Physiol. 152A, 139-148.

Nakatsuji, T., Sonobe, H., 2004. Regulation of ecdysteroid secretion from the Y-organ by molt-inhibiting hormone in the American crayfish, *Procambarus clarkii*. Gen. Comp. Endocrinol. 135, 358-364.

Nakatsuji, T., Sonobe, H., Watson, R.D., 2006. Molt-inhibiting hormone-mediated regulation of ecdysteroid synthesis in Y-organs of the crayfish (*Procambarus clarkii*): involvement of cyclic GMP and cycle nucleotide phosphodiesterase. Molec. Cell. Endocrinol. 253, 76-82.

Nighorn, A., Byrnes, K.A., Morton, D.B., 1999. Identification and characterization of a novel beta subunit of soluble guanylyl cyclase that is active in the absence of a second subunit and is relatively insensitive to nitric oxide. J. Biol. Chem. 274, 2525-2531.

Nighorn, A., Gibson, N.J., Rivers, D.M., Hildebrand, J.G., Morton, D.B., 1998. The nitric oxide-cGMP pathway may mediate communication between sensory afferents and projection neurons in the antennal lobe of *Manduca sexta*. J. Neurosci. 18, 7244-7255.

Nighorn, A., Simpson, P.J., Morton, D.B., 2001. The novel guanylyl cyclase MsGC-I is strongly expressed in higher-order neuropils in the brain of *Manduca sexta*. J. Exp. Biol. 204, 305-314.

Pavloff, M.S., Goy, M.F., 1990. Purification and chemical characterization of peptide-G1, an invertebrate neuropeptide that stimulates cyclic GMP metabolism. J. Neurochem. 55, 788-797.

Reid, D.G., Abello, P., Kaiser, M.J., Warman, C.G., 1997. Carapace colour, inter-moult duration and the behavioural and physiological ecology of the shore crab *Carcinus maenas*. Estuar. Coast. Shelf Sci. 44, 203-211.

Santos, E.A., Keller, R., 1993. Crustacean hyperglycemic hormone (CHH) and the regulation of carbohydrate metabolism: Current perspectives. Comp. Biochem. Physiol. 106A, 405-411.

Sefiani, M., Le Caer, J.P., Soyez, D., 1996. Characterization of hyperglycemic and molt-inhibiting activity from sinus glands of the penaeid shrimp *Penaeus vannamei*. Gen. Comp. Endocrinol. 103, 41-53.

Serrano, L., Blanvillain, G., Soyez, D., Charmantier, G., Grousset, E., Aujoulat, F., Spanings-Pierrot, C., 2003. Putative involvement of crustacean hyperglycemic hormone isoforms in the neuroendocrine mediation of osmoregulation in the crayfish *Astacus leptodactylus*. J. Exp. Biol. 206, 979-988.

Simpson, P.J., Nighorn, A., Morton, D.B., 1999. Identification of a novel guanylyl cyclase that is related to receptor guanylyl cyclases, but lacks extracellular and transmembrane domains. J. Biol. Chem. 274, 4440-4446.

Skinner, D.M., 1985. Molting and regeneration. In: Bliss, D.E., Mantel, L.H. (Eds.), The Biology of Crustacea, Academic Press, New York, pp. 43-146

Soyez, D., Van Herp, F., Rossier, J., Le Caer, J.P., Tensen, C.P., Lafont, R., 1994. Evidence for a conformational polymorphism of invertebrate neurohormones. D-

amino acid residue in crustacean hyperglycemic peptides. J. Biol. Chem. 269, 18295-18298.

Webster, S.G., 1991. Amino acid sequence of putative moult-inhibiting hormone from the crab *Carcinus maenas*. Proc. R. Soc. Lond. [Biol.] 244, 247-252.

Webster, S.G., 1998. Neuropeptides inhibiting growth and reproduction in crustaceans. Soc. Exp. Biol. 65, 33-52.

Yang, W.J., Aida, K., Nagasawa, H., 1997. Amino acid sequences and activities of multiple hyperglycemic hormones from the Kuruma prawn, *Penaeus japonicus*. Peptides 18, 479-485.

Yasuda, A., Yasuda, Y., Fujita, T., Naya, Y., 1994. Characterization of crustacean hyperglycemic hormone from the crayfish (*Procambarus clarkii*): Multiplicity of molecular forms by stereoinversion and diverse functions. Gen. Comp. Endocrinol. 95, 387-398.

Zheng, J.Y., Lee, C.Y., Watson, R.D., 2006. Molecular cloning of a putative receptor guanylyl cyclase from Y-organs of the blue crab, *Callinectes sapidus*. Gen. Comp. Endocrinol. 146, 329-336.

Table 1. Primers used for cloning partial cDNA encoding *C. maenas* guanylyl cyclases

Nested PCR	
Cm-GC-deg OF3	TAY AAR GTG GAG ACH RTV GG
Cm-GC-degOR3	GGA AAS AGR CAR TAD CMH GGC
Cm-GC-degIF4	AAR GTG GAG ACH RTV GGS GA
Cm-GC-degIR4	AAS AGR CAR TAD CMH GGC AT
PCR	
F1 GCII 3'RACE	CTG TTG GAC GCC ATC AAC
F2 GCII 3'RACE	CTA CCT ATC CGT AAC GAG GAG C
F13 GCII	CCC ACC ATC TTC GAC AAC ATC CTG
R7 GCII	GTT ACG GAT AGG TAG CCC GCT TAC
3' RACE	
F1 GCI	CAC CAT CGG CAT CCA CAC
F2 GCI	CAC GCC AAG TGC ATC GGC
F1 GCIII	CTT CAC CAT TGC TCA CCG TC
F2 GCIII	GAC GCA TAC ATG GTG GTA TC

Table 2. Primers used for quantifying *Cm-NOS, Cm-EF2, Cm-GCIβ, Cm-GCII*, and *Cm-GCIII*.

Primer	Sequence	Product Size
Cm-NOS F4	GTG TGG AAG AAG AAC AAG GAC G	158 bp
Cm-NOS R1	CCA CCA TCC TCT ATG CCA CAG A	
Cm-EF2 F1	CCA TCA AGA GCT CCG ACA ATG AGC G	278 bp
Cm-EF2 R1	CAT TTC GGC ACG GTA CTT CTG AGC G	
Cm-GCIβ F8	CAA GAT GAT GGG TTC GCC TTC ACC TAC C	150 bp
Cm-GCIβ R7	CTC TCT CTG GTC GTG TCT CTG CCT C	
Cm-GCII F3	CGG TGG GTG GTG AAG ATC AG	375 bp
Cm-GCII R3	CTC CGC CCA GCA CTC CGT C	
Cm-GCIII F7	GTG TGC CGT TAC TAG ACG AGA AAT ACG C	259 bp
Cm-GCIII R8	CCT CCT CAC ACA AAG ACT CCA ACG C	

FIGURE LEGENDS

Figure 1. Nucleotide and amino acid sequences of cDNA encoding *C. maenas* GC-Iβ. Partial sequence within the catalytic domain was obtained for three *C. maenus* guanylyl cyclases using nested degenerate primers (Table 1) directed toward the catalytic domain of land crab (DQ355433). The 3' UTR was sequenced for GCIβ using 3'RACE PCR specific forward primers (Table 1).

Figure 2. Nucleotide and amino acid sequences of cDNAs encoding *C. maenas* GC-II.

Partial sequence within the catalytic domain was obtained for three *C. maenus* guanylyl cyclases using nested degenerate primers (Table 1) directed toward the catalytic domain of land crab (DQ355433) **(A)**. Partial GC-II sequence was obtained from the annealing of 3'RACE PCR specific forward primers to a rich poly-A sequence within the ORF (Table 1) **(B)**.

Figure 3. Nucleotide and amino acid sequences of cDNA encoding *C. maenas* GC-III.

Partial sequence within the catalytic domain was obtained for three *C.maenus* guanylyl cyclases using nested degenerate primers (Table 1) directed toward the catalytic domain of land crab (DQ355433). The 3' UTR sequence for GC-III was obtained using 3'RACE PCR specific forward primers. Additional 5'sequence for *Cm-GCIII* was amplified using sequence-specific *Cm-GCII* gap bridging primers (Table 1). The primer sequences

designed were similar enough that they were able to anneal non-specifically to *Cm-GCIII*.

Figure 4. Comparison of amino acid sequences of Cm-GC-Iβ and Gl-GC-Iβ.

Cm-GC-Iβ and *Gl- GC-Iβ* (DQ355433) sequences were aligned using Clustal X software. Identity is indicated by black shading; similarity in the alignments is represented by gray shading. *Cm-GC-Iβ and Gl-GC-Iβ* share 97% identity within their amino acid sequences.

Figure 5. Comparison of amino acid sequences of Cm-GC-II and Gl-GC-II .

Cm-GC-II and *Gl- GC-II* (DQ355435) sequences were aligned using Clustal X software. Identity in alignments is indicated by black shading; similarity in the alignments is represented by gray shading. Upstream sequence has an amino acid sequence 60% identity to that of *Gl-GC-II*. The downstream sequences share a 78% identity.

Figure 6. Comparison of amino acid sequences of Cm-GC-III and Gl-GC-III.

Cm-GC-III and *Gl- GC-III* (DQ355438) sequences were aligned using Clustal X software. Identity in alignments is indicated by black shading; similarity in the alignments is represented by gray shading. *Cm-GC-III and Gl-GC-III* share 85% identity between their amino acid sequences.

Figure 7. Effect of eyestalk ablation on hemolymph ecdysteroid concentration. Hemolyph ecdysteroid concentration was quantified by ELISA. Data are presented as hemolymph ecdysteroid (pg/µl) as a function of days post eyestalk ablation (mean ± 1 S.E.M, n =3-13).

Figure 8. Effect of eyestalk ablation on expression of *Cm-EF2* inY-organs from red and green morphs. Data are presented as log transcript copy number/µg total RNA as a function of days post ESA (A) or a function of hemolymph ecdysteroid concentration (B). Real time PCR was used to quantify mRNA levels of data in A presented as means ± 1 S.E.M (red morph n=28-29; green morph n=33).

Figure 9. Effect of eyestalk ablation on expression of *Cm-NOS, Cm-GC-Iβ, Cm-GC-II*, and *Cm-GC-III* in Y-organs. Data are presented as log transcript copy number/µg total RNA as a function of days post ESA (A, C, E, G) or a function of hemolymph ecdysteroid concentration (B, D, F, H). Real time PCR was used to quantify mRNA levels of data in A, C, E, G presented as means ± 1 S.E.M (red morph n=28-29; green morph n=33).

Figure 9. Comparison of molt stage in green morphs undergoing natural molts. Data are presented as a mean ± 1 S.E.M of log transcript copy number/µg total RNA as a function of molt stage; intermolt (n=19-10), premolt (n=8), and postmolt (n=3-4) for *Cm-NOS, Cm-GC-Iβ, Cm-GC-II*, and *Cm-GC-III*.

Figure 1.

```
accatcggcatccacacgggcgaagtagtgacgggctactgtctatttggcaacactgtc :60
 T  I  G  I  H  T  G  E  V  V  T  G  Y  C  L  F  G  N  T  V  :20
aacatcacctcgaggacggagacgacgggcgagaagggacgagtcaacgtgtctgaagtg :120
 N  I  T  S  R  T  E  T  T  G  E  K  G  R  V  N  V  S  E  V  :40
tcgtacaggtatctgcagcagccggagaaccaagatgatgggttcgccttcacctaccgc :180
 S  Y  R  Y  L  Q  Q  P  E  N  Q  D  D  G  F  A  F  T  Y  R  :60
ggtcctgtgcctatgaagggaaggaaggagcccatgcaggtgtggttcctcagcaggcgg :240
 G  P  V  P  M  K  G  R  K  E  P  M  Q  V  W  F  L  S  R  R  :80
aaggcaacgtgaggtgaagaagcaggacaagatggaggcagagacacgaccagagagaga :300
 K  A  T                                                     :83
aaaaaaaaaaaacctatagtgagtcgtattaattcggatccgcg                 :344
```

Figure 2. A.

```
gtgtgtacggttaccgagtactgctcccgtggctccctcaaggacattctggacaacgag  :60
 V  C  T  V  T  E  Y  C  S  R  G  S  L  K  D  I  L  D  N  E   :20
gacgtgaagcttgacaacatgttcatagcttcactaattggagacatcgtgcagggtatg  :120
 D  V  K  L  D  N  M  F  I  A  S  L  I  G  D  I  V  Q  G  M   :40
atctaccttcacgattcccccgttaagtcccacggtaacctcaagtcatccaactgcctg  :180
 I  Y  L  H  D  S  P  V  K  S  H  G  N  L  K  S  S  N  C  L   :60
gtggattcccggtgggtggtgaagatcagtgactttgggcttcacgaacttaagtcaggc  :240
 V  D  S  R  W  V  V  K  I  S  D  F  G  L  H  E  L  K  S  G   :80
tatgaaacaacatcagtggcggaggcgggcgagacgcagaggaggtgtacagacctgctg  :300
 Y  E  T  T  S  V  A  E  A  G  E  T  Q  R  R  C  T  D  L  L   :100
taccgtgcccctgagctgctgagggacacgtcggcgccccctggagggacgcagaagggc  :360
 Y  R  A  P  E  L  L  R  D  T  S  A  P  P  G  G  T  Q  K  G   :120
gacgtgtactccttcgccatcatcctctacgaagttcacgtacgccacggcccctggggc  :420
 D  V  Y  S  F  A  I  I  L  Y  E  V  H  V  R  H  G  P  W  G   :140
gccacggaccaaagccccttgtccgtgattcgcctggtgatggcgggcgtacaaggctca  :480
 A  T  D  Q  S  P  L  S  V  I  R  L  V  M  A  G  V  Q  G  S   :160
aactctcccgtgagaccgtctgtggaagctatggggagttctctggactgtgtgcgtgtg  :540
 N  S  P  V  R  P  S  V  E  A  M  G  S  S  L  D  C  V  R  V   :180
gtgctgacggagtgctgggcggaggtacccgaggagaggccggacttcaggagcgtcaag  :600
 V  L  T  E  C  W  A  E  V  P  E  E  R  P  D  F  R  S  V  K   :200
atcaagctcagacccatgaggaaaggactgaagcccaacatcttcgacaacatgctgaaa  :720
 I  K  L  R  P  M  R  K  G  L  K  P  N  I  F  D  N  M  L  K   :240
aaaaaaaacctatagtgagtcgtattaattcggatccg                        :759
 K  K  N  L  -  -  V  V  L  I  R  I                           :252
```

Figure 2. B.

```
aaggtggagactgtcggggacgcgtacatggtggtaagcgggctacctatccgtaacgag  :60
 K  V  E  T  V  G  D  A  Y  M  V  V  S  G  L  P  I  R  N  E   :20
gagcagcacgccggagaggtcgcgtccatgtccctccacctgttggacgccatcaacaag  :120
 E  Q  H  A  G  E  V  A  S  M  S  L  H  L  L  D  A  I  N  K   :40
ttccagatccgccaccgtcccacagacaccctcaagcttcgtattggactccactcaggt  :180
 F  Q  I  R  H  R  P  T  D  T  L  K  L  R  I  G  L  H  S  G   :60
ccagtgtgtgcaggcgtggtgggactcaagatgccgtgatactgcctgt             :240
 P  V  C  A  G  V  V  G  L  K  M  P  -  Y  C  L               :80
```

Figure 3.

```
cccaacatcttcgacaacatgctggaaatgatggaaaagtacgccaataatctcgaggct :60
 P  N  I  F  D  N  M  L  E  M  M  E  K  Y  A  N  N  L  E  A  :20
ctagtggatgagagaacggaccagctcatccaggagaagaagaaaacagaggcgctgctg :120
 L  V  D  E  R  T  D  Q  L  I  Q  E  K  K  K  T  E  A  L  L  :40
tacgagatgctgccgccctatgtggctgaacagctcaagaggggacgcaaggtacaggct :180
 Y  E  M  L  P  P  Y  V  A  E  Q  L  K  R  G  R  K  V  Q  A  :60
gagagcttcgactgtgtcaccatctacttcagtgacattgtgggattcactgagatgtcc :240
 E  S  F  D  C  V  T  I  Y  F  S  D  I  V  G  F  T  E  M  S  :80
gctgagtcaacgcccatgcaggtggtgcatctcctcaacgacctttacacacgcttcgac :300
 A  E  S  T  P  M  Q  V  V  H  L  L  N  D  L  Y  T  R  F  D  :100
gctatcatcgagaacttcgacgtgtacaaggtggagactgtgggggacgcatacatggtg :360
 A  I  I  E  N  F  D  V  Y  K  V  E  T  V  G  D  A  Y  M  V  :120
gtatccggacttccggtgaggaacggcactacacacacaagagagatcgcgaggatgtcc :420
 V  S  G  L  P  V  R  N  G  T  T  H  T  R  E  I  A  R  M  S  :140
ttggcgctgctgcaagaggtagataccttcaccattgctcaccgtcctgaccacaaactg :480
 L  A  L  L  Q  E  V  D  T  F  T  I  A  H  R  P  D  H  K  L  :160
aagctgaggatcgggatgcacacgggaccctgcgtggctggtgtggtgggcctcaaaatg :540
 K  L  R  I  G  M  H  T  G  P  C  V  A  G  V  V  G  L  K  M  :180
ccttgatactgcctgttcggcgacactgtcaacactgcctcgcggatggagagtaatgga :600
 P  -  Y  C  L  F  G  D  T  V  N  T  A  S  R  M  E  S  N  G  :200
caaccactgaagatccatgtatccccctgcacccagaagttgttggctgagcactacccc :660
 Q  P  L  K  I  H  V  S  P  C  T  Q  K  L  L  A  E  H  Y  P  :220
tccttcgtgttggagcttcgtggagaggttgacatgaagggcaaagggaggatgtacacc :720
 S  F  V  L  E  L  R  G  E  V  D  M  K  G  K  G  R  M  Y  T  :240
tactggttgcttggggagaacgattctggagcttaaggcaaagggaggatgtacacctac :780
 Y  W  L  L  G  E  N  D  S  G  A                              :251
tggttgcttggggagaacgattctggagcttaaggtgcaccatttcctcctcacacaaag :840
actccaacgcccagctggccactgtctctggctccacgcctccgccgctctgggtcgtag :900
catccgccgctcttgagaagcccatcactagaatatggactcaagaatccccttcccttc :960
agtttccaggcaccgcgacgcagccctcacgccttgcaccgtagcgctctcctcaacccg :1020
gcattaccgaaagcttgcaagatgtttataagccttgcgtatttctcgtctagtaacggc :1080
acacatgtgcgggattcagtaggatattgaatactataatgttctatgatagatgctcat :1140
tgaagaaaaaaaaaaaacctatagtgagtcgtattaattcggatccgcg             :1189
```

Figure 4.

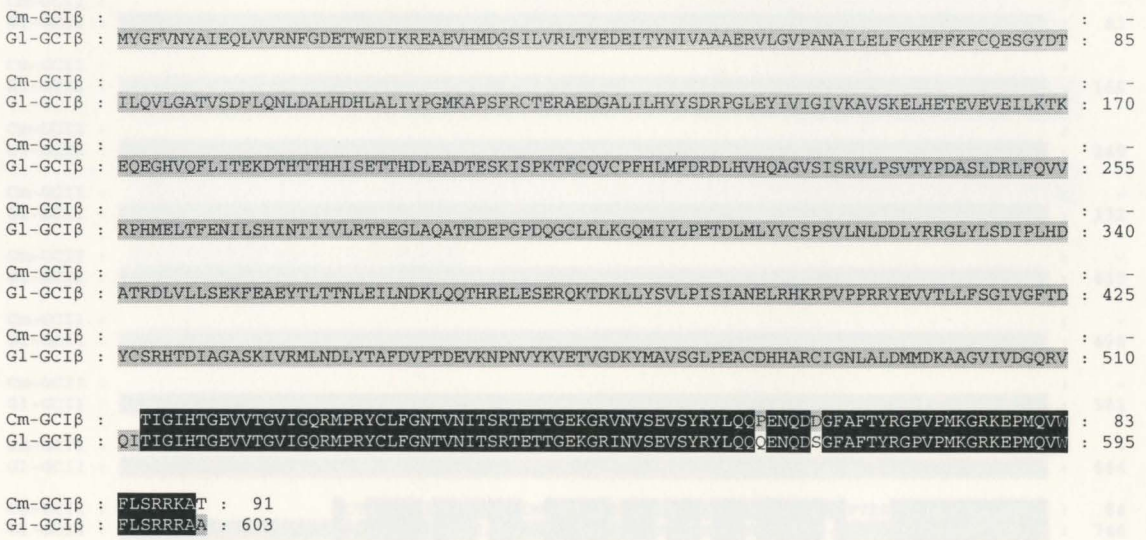
Cm-GCIβ :
Gl-GCIβ : MYGFVNYAIEQLVVRNFGDETWEDIKREAEVHMDGSILVRLTYEDEITYNIVAAAERVLGVPANAILELFGKMFFKFCQESGYDT : 85
Cm-GCIβ :
Gl-GCIβ : ILQVLGATVSDFLQNLDALHDHLALIYPGMKAPSFRCTERAEDGALILHYYSDRPGLEYIVIGIVKAVSKELHETEVEVEILKTK : 170
Cm-GCIβ :
Gl-GCIβ : EQEGHVQFLITEKDTHTTHHISETTHDLEADTESKISPKTFCQVCPFHLMFDRDLHVHQAGVSISRVLPSVTYPDASLDRLFQVV : 255
Cm-GCIβ :
Gl-GCIβ : RPHMELTFENILSHINTIYVLRTREGLAQATRDEPGPDQGCLRLKGQMIYLPETDLMLYVCSPSVLNLDDLYRRGLYLSDIPLHD : 340
Cm-GCIβ :
Gl-GCIβ : ATRDLVLLSEKFEAEYTLTTNLEILNDKLQQTHRELESERQKTDKLLYSVLPISIANELRHKRPVPPRRYEVVTLLFSGIVGFTD : 425
Cm-GCIβ :
Gl-GCIβ : YCSRHTDIAGASKIVRMLNDLYTAFDVPTDEVKNPNVYKVETVGDKYMAVSGLPEACDHHARCIGNLALDMMDKAAGVIVDGQRV : 510
Cm-GCIβ : TIGIHTGEVVTGVIGQRMPRYCLFGNTVNITSRTETTGEKGRVNVSEVSYRYLQQPENQDDGFAFTYRGPVPMKGRKEPMQVW : 83
Gl-GCIβ : QITIGIHTGEVVTGVIGQRMPRYCLFGNTVNITSRTETTGEKGRINVSEVSYRYLQQQENQDSGFAFTYRGPVPMKGRKEPMQVW : 595
Cm-GCIβ : FLSRRKAT : 91
Gl-GCIβ : FLSRRRAA : 603

Figure 5.

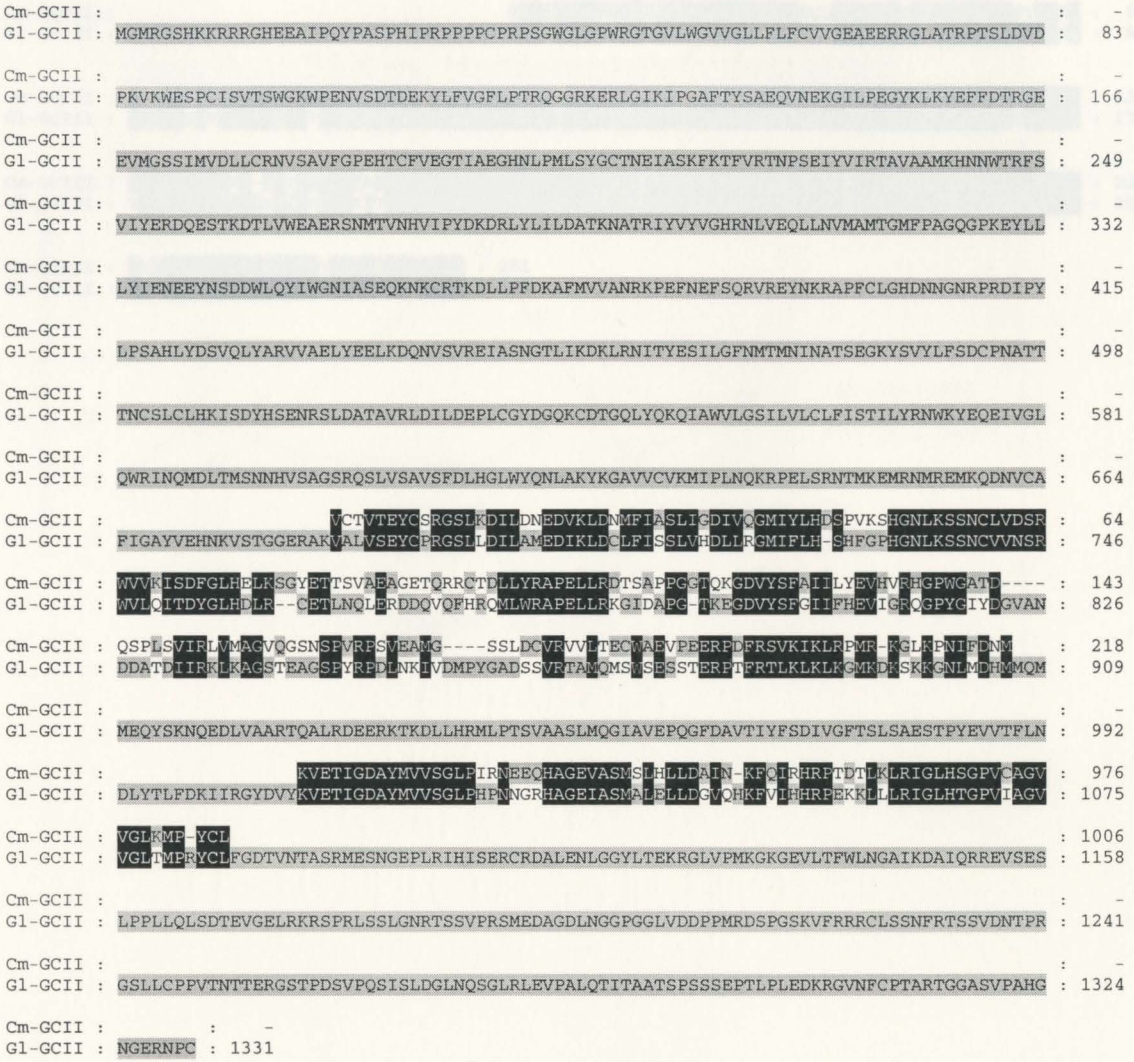

Figure 6.

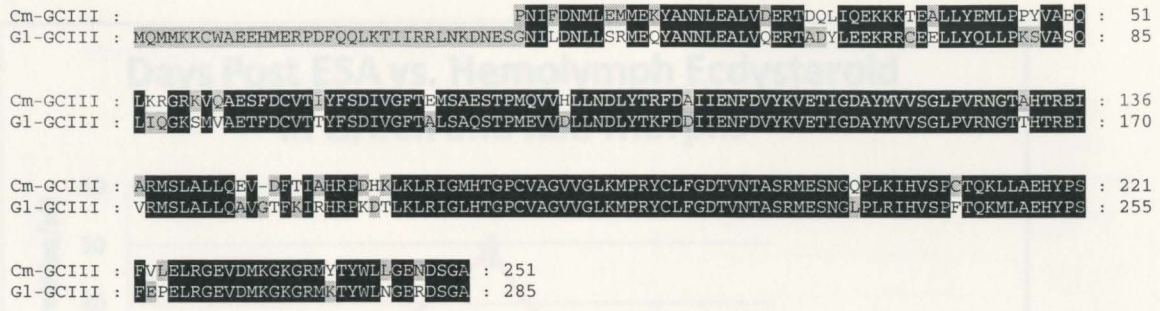
Cm-GCIII : PNIFDNMLEMMEKYANNLEALVDERTDQLIQEKKKTEALLYEMLPPYVAEQ : 51
Gl-GCIII : MQMMKKCWAEEHMERPDFQQLKTIIRRLNKDNESGNILDNLLSRMEQYANNLEALVQERTADYLEEKRRCEELLYQLLPKSVASQ : 85
Cm-GCIII : LKRGRKVQAESFDCVTIYFSDIVGFTEMSAESTPMQVVHLLNDLYTRFDAIIENFDVYKVETIGDAYMVVSGLPVRNGTAHTREI : 136
Gl-GCIII : LIQGKSMVAETFDCVTTYFSDIVGFTALSAQSTPMEVVDLLNDLYTKFDIIENFDVYKVETIGDAYMVVSGLPVRNGTTHTREI : 170
Cm-GCIII : ARMSLALLQEV-DFTTAHRPDHKLKLRIGMHTGPCVAGVVGLKMPRYCLFGDTVNTASRMESNGQPLKIHVSPQTQKLLAEHYPS : 221
Gl-GCIII : VRMSLALLQAVGTFKTRHRPKDTLKLRIGLHTGPCVAGVVGLKMPRYCLFGDTVNTASRMESNGLPLRIHVSPFTQKMLAEHYPS : 255
Cm-GCIII : FVLELRGEVDMKGKGRMYTYWLLGENDSGA : 251
Gl-GCIII : FEPELRGEVDMKGKGRMKTYWLNGERDSGA : 285

Figure 7

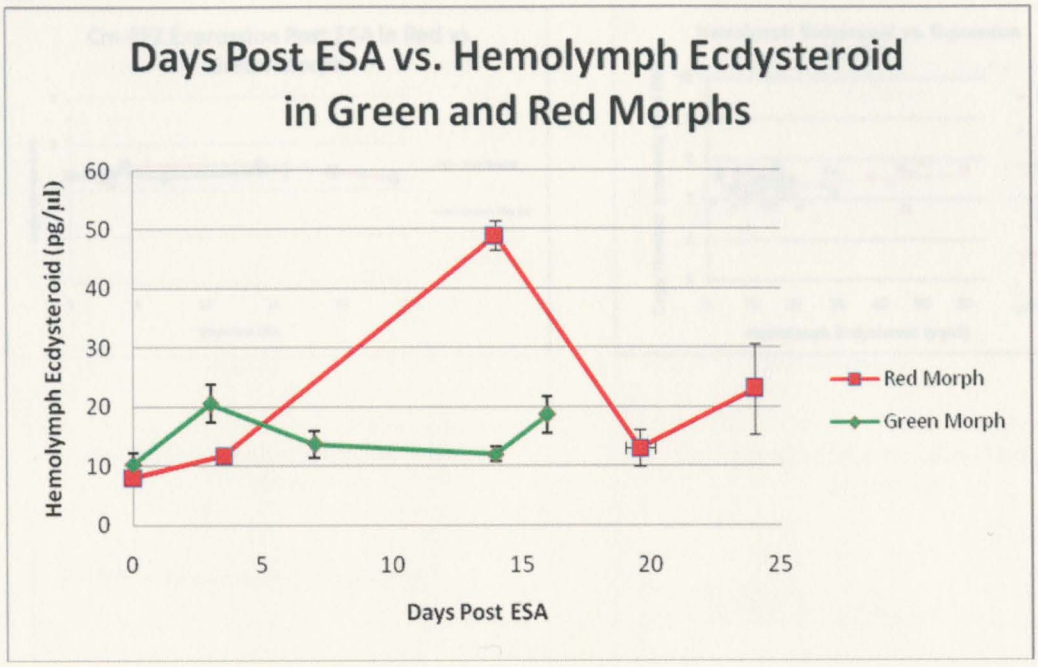
Days Post ESA vs. Hemolymph Ecdysteroid in Green and Red Morphs
Hemolymph Ecdysteroid (pg/µl)
60
50
40
30
20
10
0
0
5
10
15
20
25
Days Post ESA
Red Morph
Green Morph

Figure 8.

A.

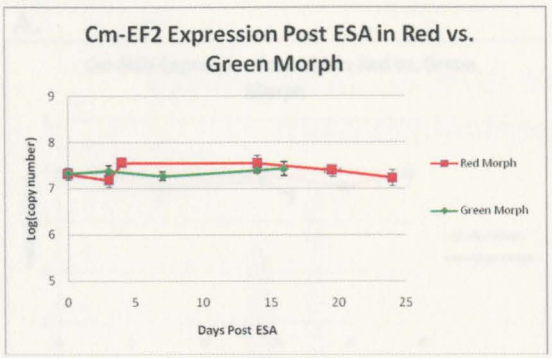
Cm-EF2 Expression Post ESA in Red vs. Green Morph
Log(copy number)
Days Post ESA
Red Morph
Green Morph

B.

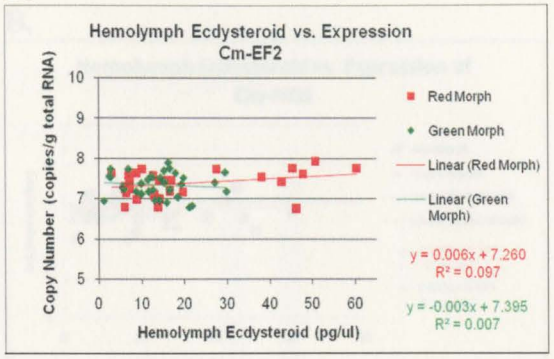
Hemolymph Ecdysteroid vs. Expression Cm-EF2
Copy Number (copies/g total RNA)
Hemolymph Ecdysteroid (pg/ul)
Red Morph
Green Morph
Linear (Red Morph)
Linear (Green Morph)
y = 0.006x + 7.260
R² = 0.097
y = -0.003x + 7.395
R² = 0.007

Figure 9

A.

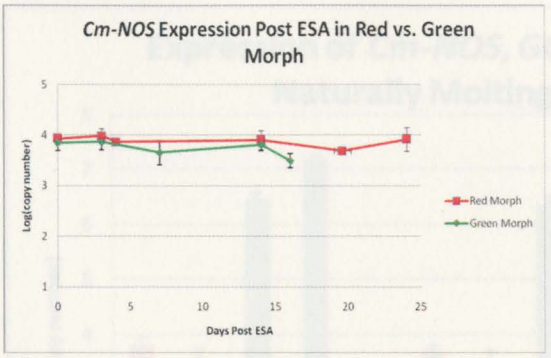

B.

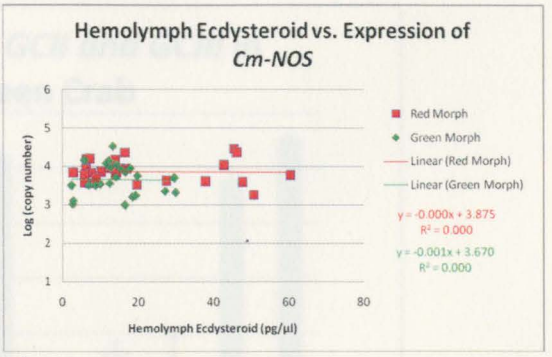

C.

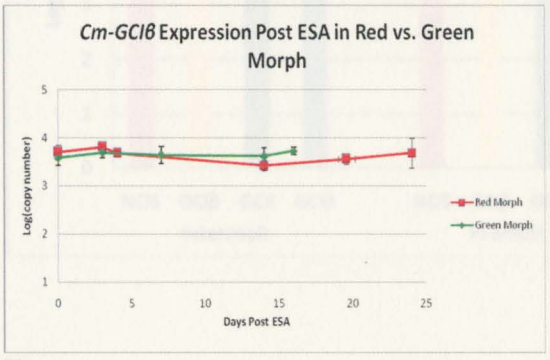

D.

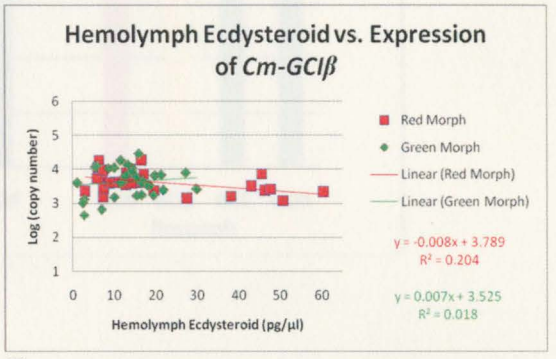

E.

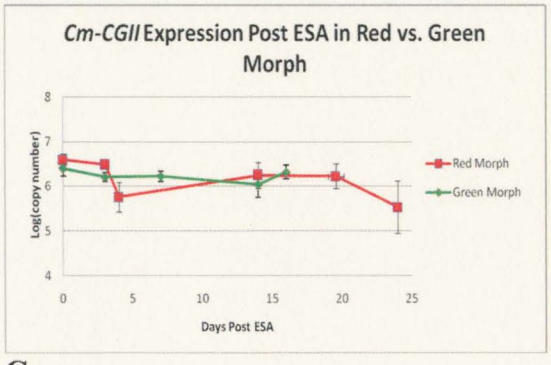

F

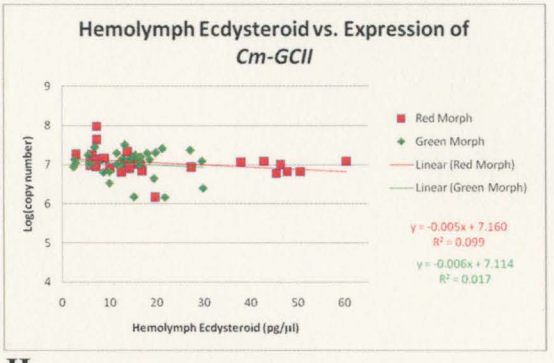

G.

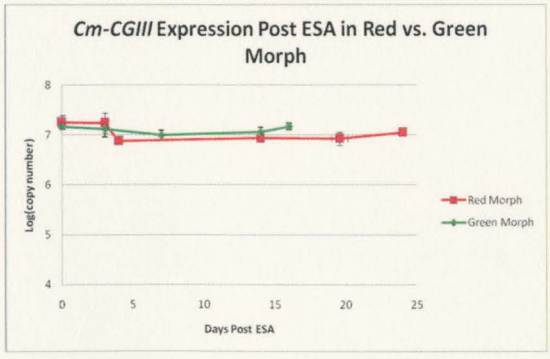

H.

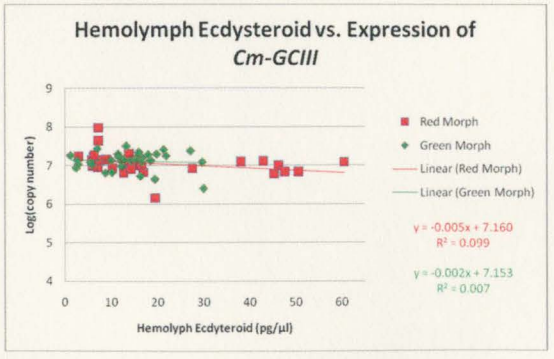

Figure 10

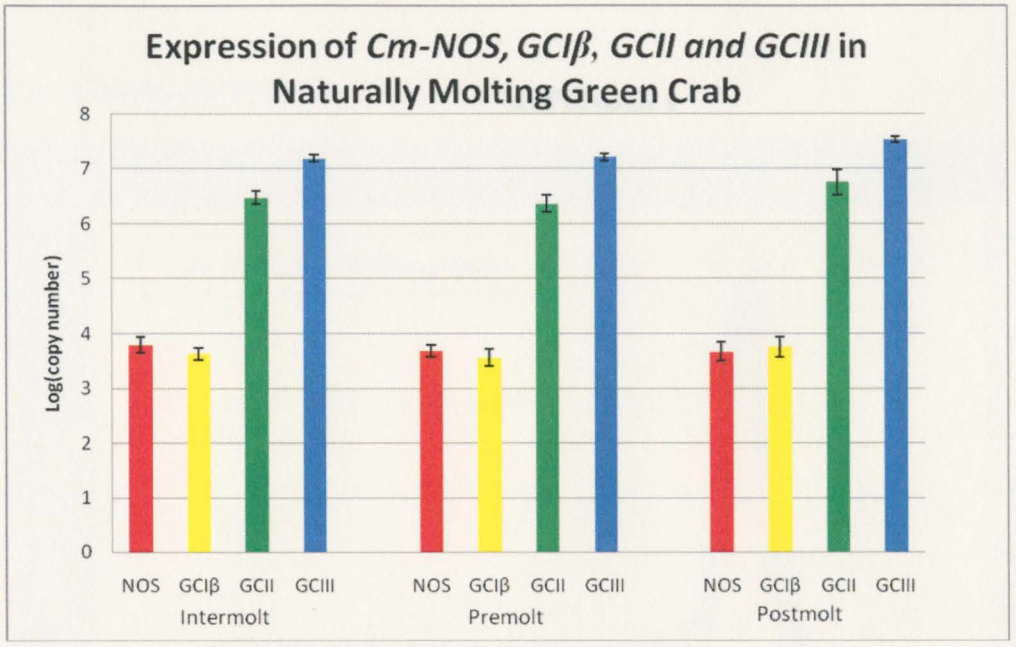
Expression of Cm-NOS, GCIß, GCII and GCIII in Naturally Molting Green Crab
Log(copy number)
0
1
2
3
4
5
6
7
8
NOS GCIβ GCII GCIII
Intermolt
NOS GCIβ GCII GCIII
Premolt
NOS GCIβ GCII GCIII
Postmolt

APPENDIX I

I. The melting peak analysis of *Cm-EF2* (A), *Cm-NOS* (B), *Cm-GC-Iβ* (C), *Cm-GC-II* (D), *Cm-GC-III* (E) was conducted using Roche, version 1.2 Light cycler 480 software.

I A. *Cm-GC-EF2* Melting Peaks

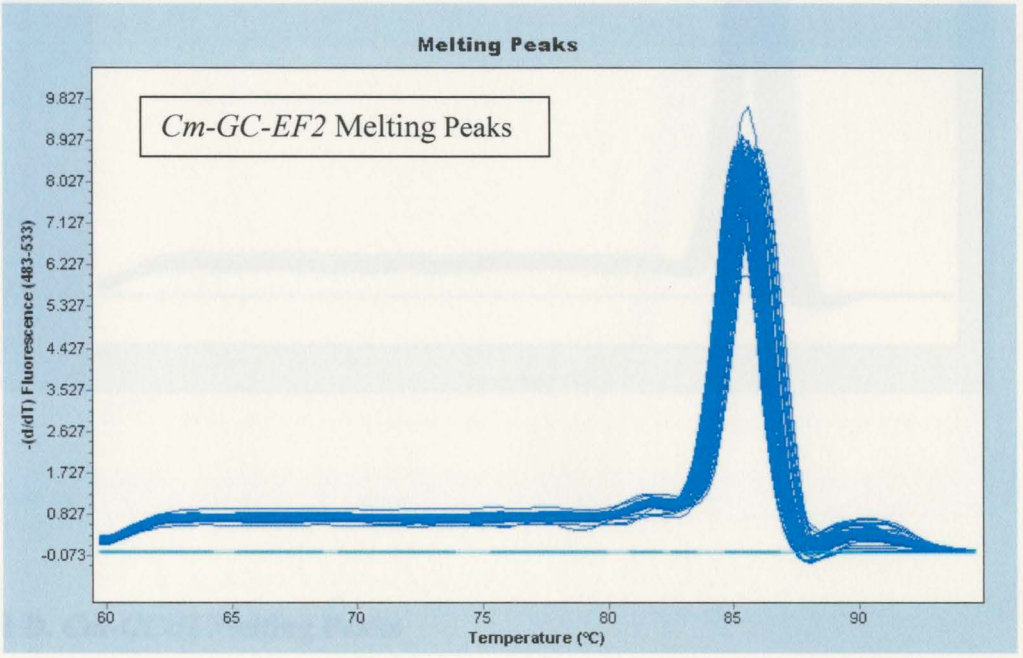

I B. *Cm-GC-NOS* Melting Peaks

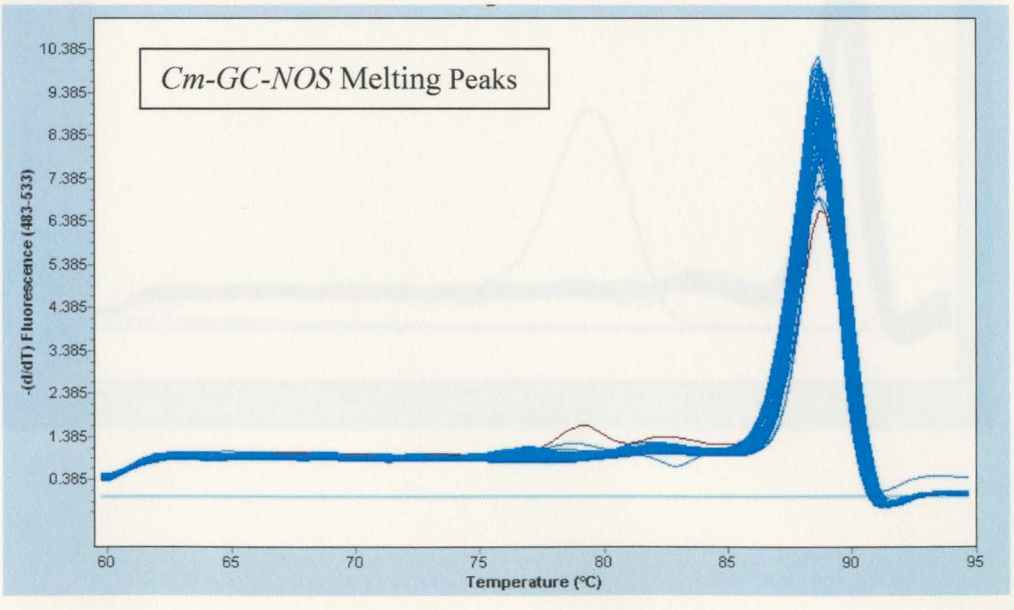

I C. *Cm-GC-Iβ* Melting Peaks

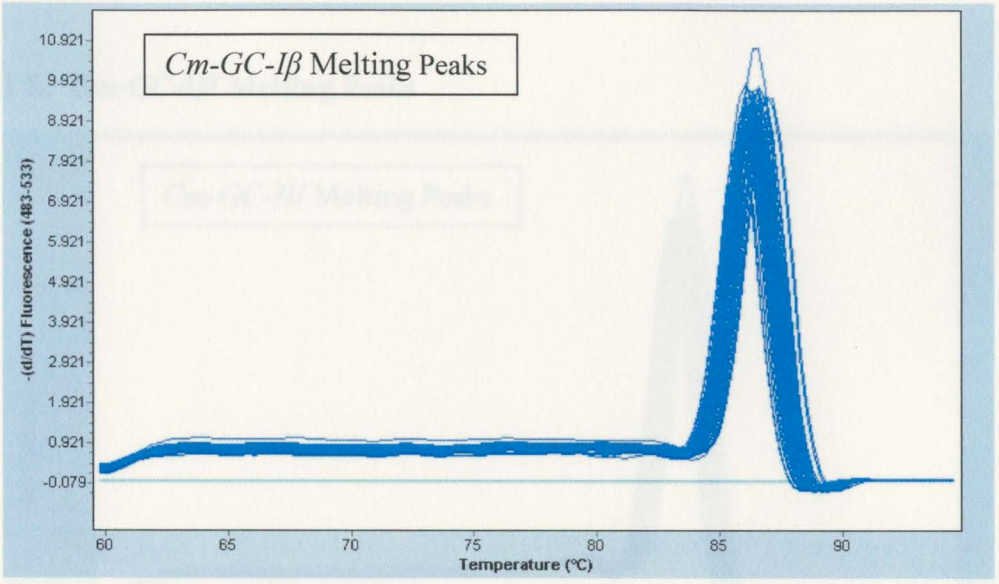

I D. *Cm-GC-II* Melting Peaks

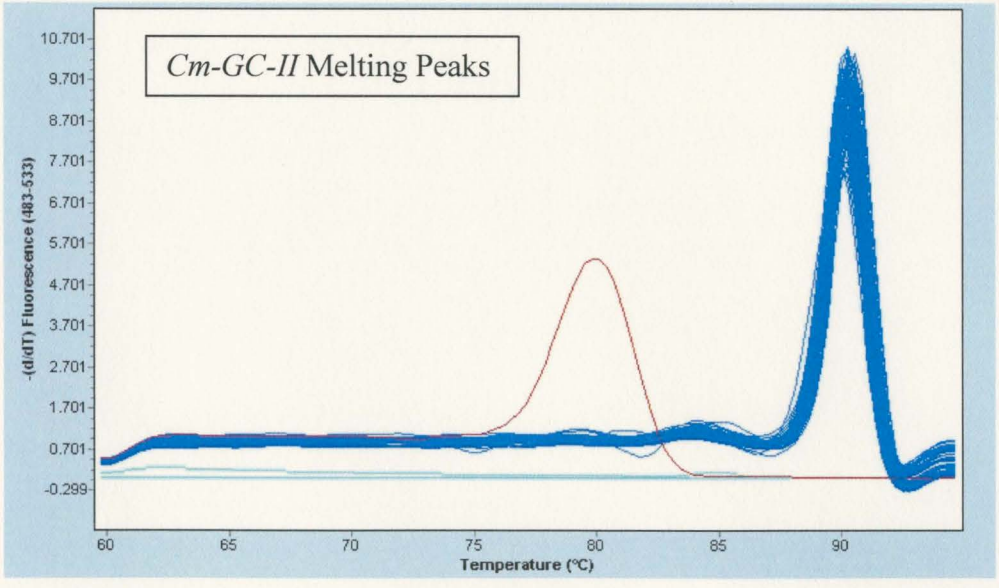

I E. *Cm-GC-III* Melting Peaks